

Viscoelasticity of Subcortical Gray Matter Structures

Curtis L Johnson¹, Hillary Schwarz¹, Matthew DJ McGarry², Bradley P Sutton¹, and Neal J Cohen¹

¹Beckman Institute for Advanced Science and Technology, University of Illinois at Urbana-Champaign, Urbana, IL, United States, ²Thayer School of Engineering, Dartmouth College, Hanover, NH, United States

INTRODUCTION: Brain tissue mechanics measured with magnetic resonance elastography (MRE) are significantly disrupted in neurodegenerative conditions, and reflect the degradation of the underlying tissue microstructure in disease [1]. Recently, investigations have focused on local stiffness measurements of specific neuroanatomical structures that are differentially affected depending on diagnosis [2,3]. In this work, we introduce a high-resolution MRE method for examining subcortical gray matter structures and present differences in viscoelasticity between the hippocampus, thalamus, and putamen in healthy young participants. While others have presented subcortical gray matter MRE measurements [2,4], our methodology is specifically designed to overcome issues arising from inadequate spatial resolution [5] and proximity to cerebrospinal fluid [6].

METHODS: We measured the mechanical properties of subcortical gray matter structures in a homogeneous population of 16 healthy volunteers (male; right-handed; 18-33 yo) using the pipeline described below. All scanning was performed using a Siemens 3T Trio with 32-channel head coil (Siemens Medical Solutions; Erlangen, Germany) and the Resoundant pneumatic actuator (Rochester, MN).

We scanned each subject using a 3D multislabs, multishot acquisition with a 1.6 mm isotropic voxel size [7] over 60 slices aligned AC-PC centered on the inferior part of the cerebrum. Vibration at 50 Hz was applied, uninterrupted, for the entire 12 minute acquisition time. Prior to estimating tissue properties, we generated masks for the bilateral hippocampus, thalamus, and putamen from a separate MPRAGE acquisition using FreeSurfer, and registered these masks to the MRE dataset with FLIRT in FSL. Along with the high-resolution displacement field, these masks were input to the nonlinear inversion algorithm (NLI; [8]) in order to promote local homogeneity using soft prior regularization (SPR; [9]). NLI returned the shear modulus, $G = G' + iG''$, from which we calculated shear stiffness, $\mu = 2|G|^2 / (G' + |G|)$, and damping ratio, $\xi = G'' / 2G'$, which describes relative tissue viscosity, in each of the three structures.

RESULTS and DISCUSSION: Figure 2 presents the stiffness of the hippocampus, thalamus, and putamen across our population, along with an example stiffness map with the structure masks outlined. Differences between structures were tested with the non-parametric Wilcoxon sign-rank test (significance: $p < 0.05$). We found that the hippocampus ($\mu: 3.37 \pm 0.38$ kPa) is softer than the thalamus ($\mu: 3.74 \pm 0.29$ kPa), and that both structures are softer than the putamen ($\mu: 3.85 \pm 0.22$ kPa). Similarly, Figure 3 presents the same comparison but for damping ratio. In this case, the putamen ($\xi: 0.21 \pm 0.01$ kPa) exhibits a greater relative viscosity than both the thalamus ($\xi: 0.19 \pm 0.01$ kPa) and hippocampus ($\xi: 0.17 \pm 0.03$ kPa). These relationships in mechanical properties reflect the inherent differences in cellular architecture between the different regions. As stiffness and viscosity are related to different microscale tissue characteristics [1], these data suggest that the high-resolution MRE measures are sensitive to this underlying microstructure and potential alterations in disease.

We also compared the variability within the population for the volume, stiffness, and damping ratio measures, with variability defined as the standard deviation over the mean (Figure 4). We found that the hippocampus showed much greater variability in MRE measures ($\mu: 11.4\%$; $\xi: 15.7\%$) than in volume (8.3%). Since we expect stiffness and viscosity to relate to tissue microstructure that ostensibly influences neurological function, the greater variability suggests that MRE produces more sensitive measures of hippocampal structure than volume. Interestingly, mechanical properties of the thalamus and putamen exhibited variability similar to the volume. Since the hippocampus is highly susceptible to change with age and some disease states, more so than the thalamus or putamen, the variability of the hippocampal MRE measures suggest that they are highly sensitive to structural degradation that manifests as volume change. It is likely that in populations expected to exhibit thalamic and putaminal atrophy, similar behavior may be found in these structures.

CONCLUSION: We presented measurements of subcortical gray matter structures in the human brain generated using a high-resolution MRE method, and showed that the hippocampus, thalamus, and putamen exhibit different viscoelasticity owing to their specific microarchitecture. We also demonstrated that these measurements appear to be more sensitive to underlying hippocampal structure than traditional volumetric measures. Ultimately, such measurements may be critical in characterizing the microstructural degradation that precedes the gross structural atrophy linked to functional decline in aging and disease.

REFERENCES: [1] I Sack, *et al.*, *Soft Matter*, 2013, 9(24):5672-5680; [2] A Lipp, *et al.*, *NeuroImage Clin*, 2013, 3:381-387; [3] AJ Romano, *Magn Reson Med*, in press; [4] J Guo, *et al.*, *PLoS ONE*, 2013, 8(8):e71807; [5] CL Johnson, *et al.*, *Magn Reson Med*, 2013, 70(2):404-412; [6] MC Murphy, *et al.*, *PLoS ONE*, 2013, 8(12):e81668; [7] CL Johnson, *et al.*, *Magn Reson Med*, 2014, 71(2):477-485; [8] MDJ McGarry, *et al.*, *Med Phys*, 2012, 39(10):6388-6396; [9] MDJ McGarry, *et al.*, *IEEE T Med Imaging*, 2013, 32(10):1901-1909.

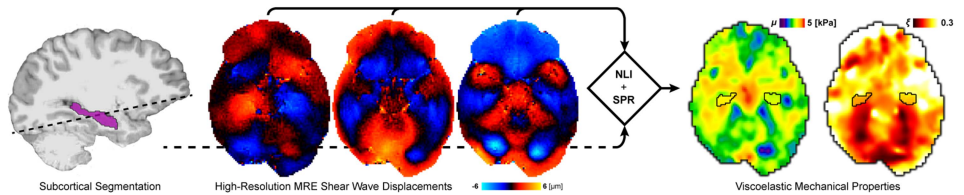


Fig. 1: MRE method incorporating high-resolution imaging and nonlinear inversion with soft prior regularization to promote local homogeneity within subcortical structures (hippocampus highlighted).

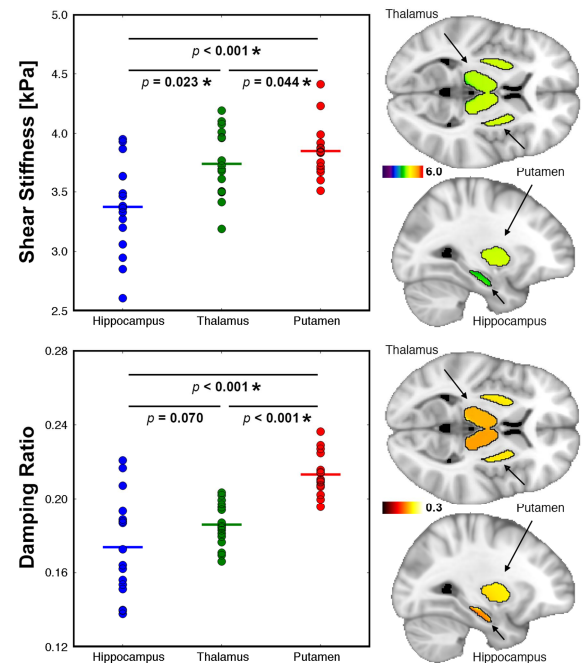


Fig. 2 (top): Stiffness values for each structure across the population, along with group averaged maps in standard space. **Fig. 3 (bottom):** The same comparison for damping ratio. Significance set at $p < 0.05$.

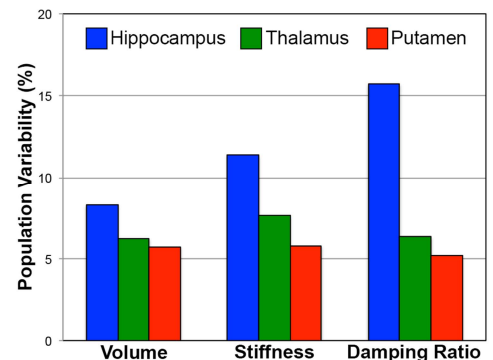


Fig. 4 (below): Population variability (st. dev. over mean) for volume, stiffness, and damping ratio.